GA–A27918

COMPARATIVE STUDIES OF STATIC EDGE MAGNETIC ISLANDS IN DIII-D AND LHD

by
T.E. EVANS, K. IDA, S. OHDACHI, K. TANAKA, M.W. SHAFER,
S. INAGAKI, M.E. AUSTIN, Y. SUZUKI, E.A. UNTERBERG,
and the LHD and DIII-D Experiment Groups

SEPTEMBER 2014

GENERAL ATOMICS

DISCLAIMER

GA–A27918

COMPARATIVE STUDIES OF STATIC EDGE MAGNETIC ISLANDS IN DIII-D AND LHD

by
T.E. EVANS, K. IDA,* S. OHDACHI,* K. TANAKA,* M.W. SHAFER,†
S. INAGAKI,‡ M.E. AUSTIN,¶ Y. SUZUKI,* E.A. UNTERBERG,†
and the LHD and DIII-D Experiment Groups

This is a preprint of a paper to be presented at the Twenty-Fifth IAEA Fusion Energy Conf., October 13-18, 2014 in Saint Petersburg, Russia.

*National Institute for Fusion Sciences, Toki Gifu, Japan.
†Oak Ridge National Laboratory, Oak Ridge, Tennessee.
‡RIAM, Kyushu University, Fukuoka, Japan.
¶University of Texas at Austin, Austin, Texas.

Work supported in part by
the U.S. Department of Energy
under DE-FC02-04ER54698, DE-AC05-00OR22725, DE-FG03-97ER54415,
and the NIFS budget code NIFS11ULHH021

GENERAL ATOMICS PROJECT 30200
SEPTEMBER 2014

Comparative Studies of Static Edge Magnetic Islands in DIII-D and LHD

T.E. Evans[1], K. Ida[2], S. Ohdachi[2], K. Tanaka[2], M.W. Shafer[3], S. Inagaki[4],
M.E. Austin[5], Y. Suzuki[2], E.A. Unterberg[3], the LHD[2] and DIII-D[1] Experiment Groups

[1]General Atomics, P.O. Box 85608, San Diego, CA 92186-5608, USA
[2]National Institute for Fusion Sciences, Toki Gifu 509-5292, Japan
[3]Oak Ridge National Laboratory, P.O. Box 2008, Oak Ridge, TN 37831, USA
[4]RIAM, Kyushu University, Kasuga, Fukuoka, 816-8580, Japan
[5]University of Texas-Austin, Austin, TX 78712-1047, USA

e-main contact of main author: evans@fusion.gat.com

Abstract. Studies of the effects of large static magnetic islands on the local energy and particle transport have been carried out in DIII-D and LHD. Measurements of changes in the time it takes for modulated electron cyclotron (MEC) heat pulses to propagate across the o-point of a *m/n*=2/1 magnetic island (τ_E^{isl}) produced by a constant DIII-D C-coil current reveal a periodic 35% change in τ_E^{isl}. These changes in τ_E^{isl} are consistent with a model in which the island spontaneously bifurcates from smooth flux surfaces to a partially stochastic region due to a nonlinear amplification of secondary resonant islands. This bifurcation of the island topology is seen in low rotation discharges with a stable *n*=1 kink mode suggesting that there is a complex nonlinear coupling between the resonant island and the kink mode. It is found that small hydrogen pellets injected into the o-point of *m/n*=1/1 magnetic islands, locked to the LHD resonant magnetic perturbation coil, transiently increase the density inside the island by a factor of 3 compared to the central density. A summary of the measurements of τ_E^{isl} in DIII-D and island particle dynamics in LHD are presented along with a discussion of the plasma response to low order magnetic islands.

1. Introduction

Knowledge of the 3D magnetic field line topology in tokamaks and stellarators is required for interpreting the physics associated with particle, energy and momentum transport when helical magnetic perturbations are present. Additionally, an understanding of the plasma response to small intrinsic and externally applied magnetic field perturbations is needed to predict and avoid the onset of MHD instabilities that can degrade the performance of the discharge or trigger abrupt discharge termination events.

In tokamaks, small 3D perturbation fields result from the application of non-axisymmetric control or correction coils and from intrinsic field-errors due to misalignments of the equilibrium field coils. In stellarators 3D perturbation fields result from misalignments of the helical equilibrium coils, axisymmetric positioning coils and from perturbation coils specifically designed to produce low-order magnetic islands embedded in the helical plasma equilibrium field. The nature of the plasma response to these small externally imposed perturbation fields is known to be sensitive to the equilibrium parameters of the discharge. For example, in the LHD heliotron-type device [1], with a relatively small helical plasma current, magnetic island widths can be large due to the low magnetic shear and are known to depend on the electron temperature, β and the position of the magnetic axis (R_{ax}) [2]. In some configurations the islands can be larger than the widths calculated using a vacuum field approximation and in other configurations islands do not appear until the amplitude of the perturbation field reaches a β dependent threshold level. In low-rotation tokamak plasmas, sustained by Ohmically induced plasma currents, visual images of static edge magnetic islands produced by an external non-axisymmetric perturbation coil agree exceptionally well

with the widths and positions of islands calculated with a vacuum field line integration code [3]. In diverted H-mode plasmas, with large edge pressure gradients and high rotation, there is as yet no conclusive experimental evidence that externally applied non-axisymmetric perturbation fields produce magnetic islands. This suggests the possibility that the plasma is capable of reducing or completely eliminating all of the resonant components produced by the perturbation field. Resolving whether or not H-mode plasmas are able to completely or partially eliminate externally applied and intrinsic resonant field components is one of the most important experimental challenges facing the development of high performance magnetic confinement plasma physics.

In this paper we discuss results from a series of experiments done by a joint team of Japanese and US scientists, the International Magnetic Island Physics (IMIP) team, on DIII-D and LHD to develop the fundamental basis needed for understanding the plasma's response to 3D magnetic field perturbations under various discharge conditions. These studies are essential for developing an understanding of the effects of magnetic islands on transport and stability and an understanding needed to interpret experiments in high performance H-mode plasmas. Two new experimental techniques have been developed by the IMIP team to test for the existence of magnetic island or stochastic layers and to assess their properties under various discharge conditions. These techniques are based on quantifying the effects of magnetic islands and stochastic layers on the heat and particle transport.

Traditionally, observations of flat spots in the radial profile of the electron temperature (T_e) are associated with the existence of static magnetic islands in stellarators [2] and stochastic layers in tokamaks [4]. Since both islands and stochastic layers produce a similar level of T_e profile flattening it is not possible to use these flat profiles to discriminate between islands and stochastic layers. On the other hand, measurements of the thermal transport across islands and stochastic layers provide unique signatures that can be used to identify one from the other. The IMIP team has deployed a novel thermal transport analysis technique to study the properties of islands and stochastic layers in DIII-D and LHD. This technique is based on measuring the time required for modulated electron cyclotron (MEC) heat pulses to propagate across flat regions in the T_e profile that are associated with either magnetic islands or stochastic layers. The method is based on a characteristic change in the local propagation time across closed flux surfaces τ_E^{cfs} compared to that of magnetic islands τ_E^{isl} and stochastic layers τ_E^{sto} where $\tau_E^{isl} > \tau_E^{sto} > \tau_E^{cfs}$ [5].

It has been shown previously that the particle transport across magnetic islands is increased due to a localized *ExB* convection inside the island o-point [6,7]. This results from an alteration of the plasma potential inside the island o-point compared to the ×-point [7]. In order to examine changes in particle transport due to magnetic islands the IMIP team has developed a technique for increasing the density inside an island and measuring the decay rate of the density perturbation. This technique is based on repetitively injecting small frozen hydrogenic pellets into the ×- and o-points of magnetic islands. Results from these experiments are compared to those with pellets injected into plasmas without magnetic islands in order to quantify changes in the density profiles.

2. DIII-D Modulated EC (MEC) Heat Pulse Experiment

In this study, elongated inner wall limited (IWL) plasmas without axisymmetric ×-points were used to maximize the diagnostic coverage and minimize the magnetic shear on the q=1 through 4 surfaces. This was done to produce the largest possible n=1 magnetic island widths on each of these rational surfaces and to optimize the diagnostic coverage in the vicinity of these islands. The plasma equilibrium shape used in these experiments is shown in Fig. 1 for shot 154526 along with the poloidal locations of the electron cyclotron emission (ECE) (blue) and Thompson scattering (red) sampling points. The location of the electron cyclotron heating (ECH) 2nd harmonic (×-mode) resonant surface is shown and the rays from the ECH launcher indicate that the power absorption takes place near ψ_N =0.2 where ψ_N is the normalized poloidal flux.

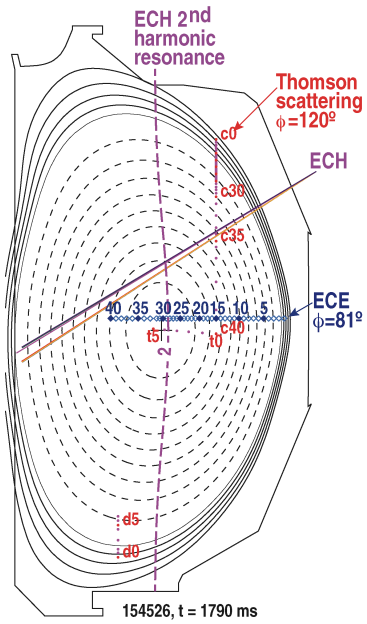

Fig. 1. Equilibrium shape used for studying the thermal transport across large magnetic islands.

This discharge had B_T = -1.92 T and I_p = 1.29 MA resulting in a q_{lim}=4.7. The neutral beams were modulated between co- and counter-sources to produce low average neutral beam injection (NBI) input power ⟨P⟩ = 1.14 MW, toroidal torque T = 0.17 Nm and pedestal rotation v_ϕ^{ped} = 12.7 kms^{-1}. This resulted in a κ=1.6 L-mode plasma with β_N=0.68. The ECH power was modulated between 3.17 MW and 0.36 MW at 50 Hz with 10 ms at the high power level and 10 ms at low power for the MEC heat pulse propagation experiment. This provided sufficiently large ECE signals and good temporal resolution for studying the properties for the heat pulse transport. The low power, low torque NBI phase started at 1000 ms and the MEC heat pulse phase at 1500 ms while the I_p plateau began at 1400 ms. An initial 300 ms period, with no externally applied n=1 C-coil resonant magnetic perturbation (RMP) field, was used to acquire reference MEC heat pulse data for calibrating the amplitude and phase of the heat pulses with nested magnetic flux surfaces.

In shot 154526, the line average density increased linearly from the initial plasma breakdown until 1735 ms when it saturated at n_e=3.97x10^{19} m^{-3}. Following the rampup of the C-coil, between 1791 and 1802 ms, the density increased again until it reached a peak value of n_e=4.45x10^{19} m^{-3} at 1970 ms. The core electron temperature T_e inside ψ_N=0.35 increased from 1.4 to 2.1 keV during the first 320 ms after applying the ECH and then dropped to 1.6 keV between 1830 and 2090 ms. The drop in n_e starting at 1970 ms was correlated with a drop in the toroidal rotation on the q=2 surface from 20 km/s to approximately 0. Prior to turning on the C-coil, q=2 is located at ψ_N =0.61 and q_{min} on axis is slightly above 1.

The RMP field from the C-coil, located on the θ=0° equatorial plane of the machine outside the vacuum vessel at $R_{C\text{-}coil}$=3.23 m with the edge of the plasma located at R_{midout}=2.24 m, was used to drive a large m/n=2/1 island with $\Delta\psi_N$=0.075 centered at ψ_N=0.074. This configuration of the C-coil also produces a m/n=1/1 vacuum island with $\Delta\psi_N$=0.15 centered at ψ_N=0.21, a m/n=3/1 island with $\Delta\psi_N$=0.05 centered at ψ_N=0.88 and a m/n=4/1 island with $\Delta\psi_N$=0.05 centered at ψ_N=0.97 as shown in Fig. 2. Intrinsic field-errors produce smaller islands such as an m/n=3/2 with $\Delta\psi_N$=0.02 centered at ψ_N=0.61. The currents in the 6 toroidal window-frame loops of the C-coil were configured for a n=1 cosine

distribution with a peak amplitude of 13.4 kAt and a toroidal phase that was modulated between $\phi_{n=1}$=5° and ϕ $\phi_{n=1}$=185° every 670 ms as shown in Fig. 3(a).

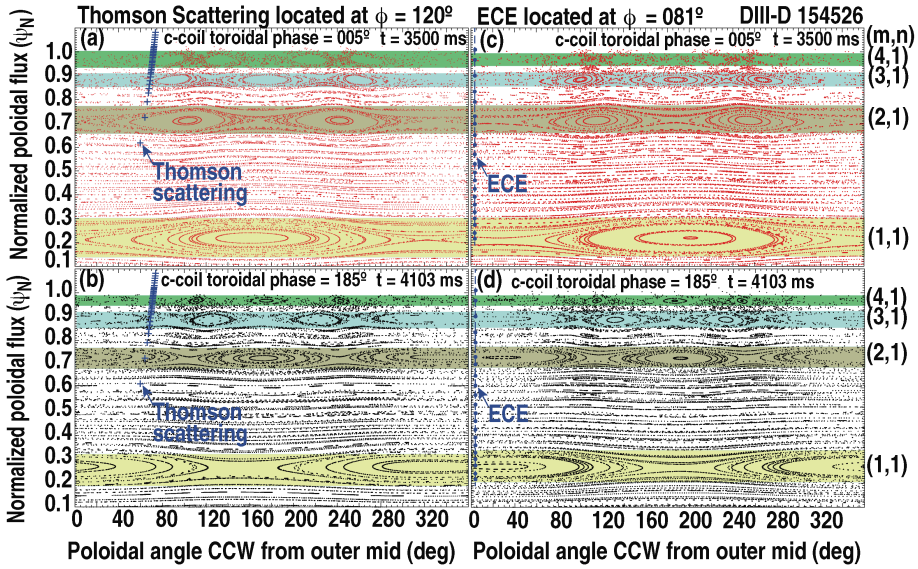

Fig. 2. Size and positions of magnetic islands calculated with the TRIP3D field line integration code [3] in shot 154526 at t=3500 ms with an n=1 C-coil phase $\phi_{n=1}$=5° and t=4301 ms with $\phi_{n=1}$=185° showing the locations of (a,b) the Thomson scattering and (c,d) the ECE sampling points with respect to each magnetic island chain without including the plasma response to the applied 3D field.

The plasma response to the applied $\phi_{n=1}$=5° field from the C-coil in this discharge starts with an initial increase in the central pressure between ψ_N=0 and ψ_N=0.3 and a drop in the toroidal rotation near q=2. This is followed by a drop in the line average density, as noted above, and a slow increase in a plasma generated poliodal field measured by a set of saddle coils located on the DIII-D vessel wall as shown in Fig. 3. Prior to the application of the C-coil field the n=2, 3 plasma fields grow at a rate of approximately 5 G/s and the n=1 field saturates near 3 G. When the C-coil field is applied the n=2, 3 fields saturate and the n=1 begins to grow at a rate of approximately 20 G/s.

When the toroidal phase of the C-coil is changed from $\phi_{n=1}$=5° and $\phi_{n=1}$=185° at 2460 ms the amplitude of the n=1 plama field at the wall is reduced by approximately 2–3 G while the growth in the amplitude of the field continues at approximately the same rate. Subsequently, the increase in the n=1 plasma field saturates by 3000 ms at an amplitude of 17 G while in the $\phi_{n=1}$=185° phase. The change in the toroidal phase of the C-coil field from $\phi_{n=1}$=185° to $\phi_{n=1}$=5° at 3130 ms causes an immediate 10 G increase in the n=1 plasma field amplitude which persists until the phase is changed back to the $\phi_{n=1}$=185° at 3860 ms. The change causes the amplitude to drop by 10 G, to its previous value in this phase. An analysis of the plasma magnetic field produced by this mode using an array of toroidal and poloidal magnetic saddle loops located on the DIII-D low-field side wall shows that it has a dominate 2/1 ballooning structure and appears to be related to a slow evolution of the equilibrium caused by a stable n=1 kink mode. It is noted that the first indication of a drop in T_e across the location indicated by the m/n=1/1 island shown in Fig. 2 takes place at 1936 ms followed by a flattening in the T_e profiles near the m/n=3/2, 2/1, and 3/1 surfaces starting at 2040 ms.

The propagation of a series of MEC heat pulses in discharge 154526, between 3900 and 4330 ms, with a C-coil phase of $\phi_{n=1}$=185° shows several spontaneous transitions in the character of the ECE signal located near the low-field side of the 2/1 island at ψ_N=0.74 compared to that at ψ_N=0.33 as seen in Fig. 4. This change in the ECE signal from a periodic modulation of the T_e locked to the MEC heat pulsed to a small somewhat incoherent fluctuation of T_e is correlated with a reduction in the time required for the MEC heat pulses to propagate across the 2/1 island as shown in Fig. 5. The ECE data shows a set of periodic transitions that indicate a series of bifurcations in the thermal transport across the 2/1 island. This bifurcation from a large coherent modulation to a smaller partially incoherent fluctuation is associated with a ~35% reduction in the time required for a heat pulse to transit the island. Figure 5 indicates an island width, measured by the MEC pulse, of $\Delta\psi_N$=0.215 centered on ψ_N=0.73. This is a factor of 2.9 larger than the width of the island shown in Fig. 2 and is consistent with the T_e profile flattening seen by the Thomson scattering and ECE diagnostics when the C-coil field is in the $\phi_{n=1}$=185 phase.

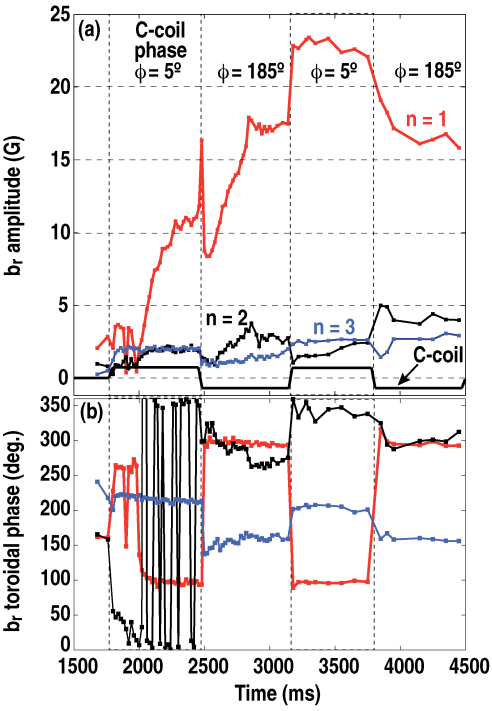

Fig. 3. (a) Amplitude and (b) toroidal phase of the poloidal component of the *n*=1 plasma generated field at DIII-D vacuum vessel wall vs time for shot 154526. The toroidal phase of the C-coil field is shown in (a).

In a discharge similar to the one shown in Fig. 1, with average NBI power $\langle P_{NBI}\rangle$ = 1.48 MW producing an average toroidal torque $\langle T\rangle$ = 0.45 Nm and with an average ECH power $\langle P_{ECH}\rangle$ = 1.35 MW, when the C-coil phase is switched from $\phi_{n=1}$=185° to $\phi_{n=1}$=5° [Fig. 6(a)] an increase in the line average density is triggered while edge toroidal rotation drops from approximately 15 km/s to 10 km/s as shown in Fig. 6(b). The average input power in this discharge is similar to that needed to trigger H-modes in a diverted discharge but the deuterium recycling does not show signatures of edge localized modes (ELMs). Instead the

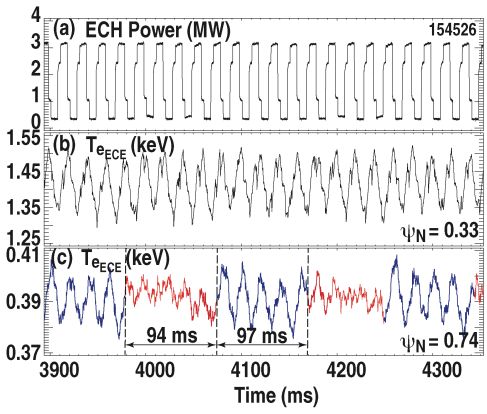

Fig. 4. (a) ECH power, (b) T_e measured by the ECE channel at ψ_N=0.33 and (c) T_e measured by the ECE channel at ψ_N=0.74.

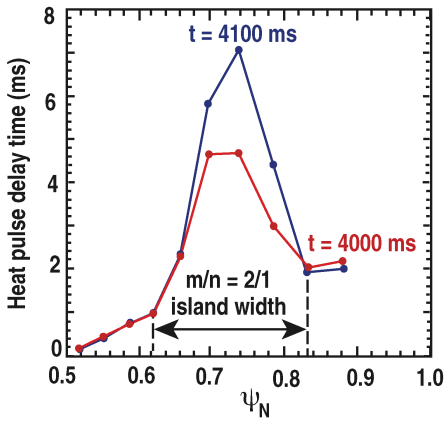

Fig. 5. MEC heat pulse propagation delay times during periodic ECE signal transitions.

recycling behavior is similar to intermittent dithering periods separated by ELM-free periods. This discharge had a significantly different kink mode and equilibrium plasma response than the one shown in Fig. 3. The n=1 plasma generated poloidal magnetic field had an average amplitude of 3.9 G in the $\phi_{n=1}$=185° phase while the n=2 and 3 radial field components were 3.0 and 6.0 G respectively. In the $\phi_{n=1}$=5° phase, during improved confinement, the n=1 field component increased to 5.8 G while the n=2 and the n=3 components did not change significantly. It is hypothesized that this change in the n=1 plasma generated magnetic field between the two toroidal phases of the C-coil perturbation field results in a nonlinear coupling between the n=1 kink mode and edge resonant field. This may explain the observed flattening of the T_e profile across the outer 2%–3% of the plasma. The improved confinement phase results in a large increase in the edge density gradient while the edge T_e gradient is relatively unchanged. This behavior is triggered by the $\phi_{n=1}$=5° C-coil phase and is similar to results seen in TORE SUPRA [8] and TEXTOR [9] experiments where improved particle confinement (IPC) modes were triggered by RMP fields.

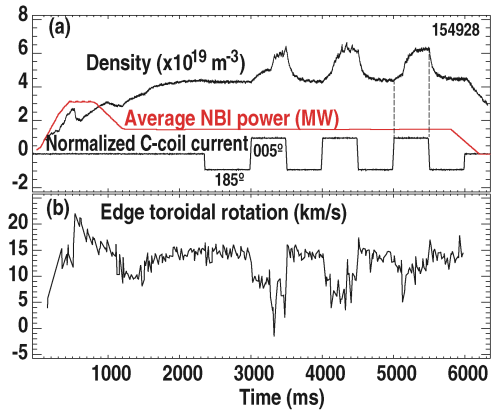

Fig. 6. (a) The line average density, average NBI power and normalized C-coil current showing density increases in the 5° phase and (b) edge toroidal rotation.

3. LHD m/n=1/1 Island Pellet Injection Experiment

Experiments done in LHD to better understand the affects of magnetic islands on particle transport have highlighted distinct differences in the particle dynamics near island o- and ×-points compared to those without an island. In these experi-ments, the RMP coil had a peak current of 1920 A and was used to produce large m/n=1/1 islands near the edge of a helium plasma with R_{ax} = 3.6 m and B_T = 2.75 T. As shown in Fig. 7, the island width is $\Delta R \cong 0.2$ m with the center of the o-point located at R=4.34 m. Small hydrogen pellets were injected at ϕ_{pel}=72° into discharges without islands or into discharges with either an island o- or ×-point positioned at the pellet injection point. The pellet ablation light (H_α) for each configuration is shown in Fig. 7(a-c) and the equilibrium flux surfaces (red) with the magnetic island

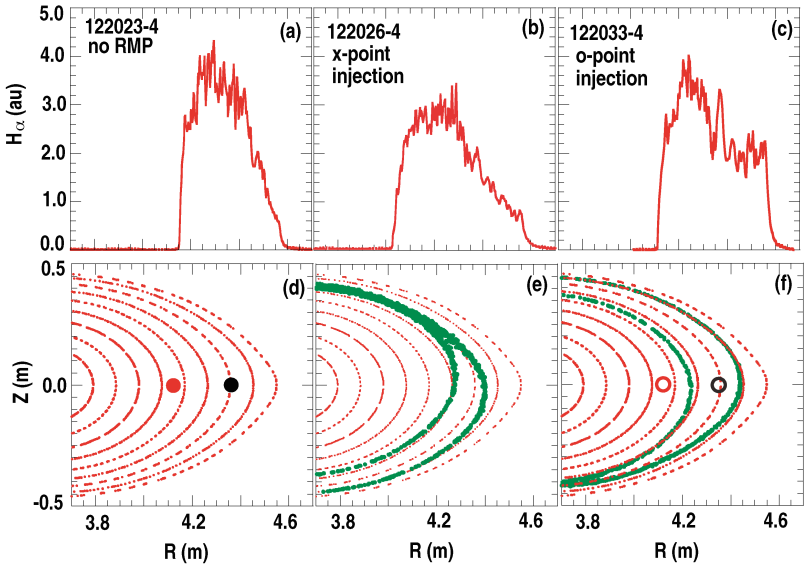

Fig. 7. Hydrogen pellet ablation light versus plasma radius for (a,d) a discharge without an island, (b,e) into the ×-point and (c,f) into the o-point.

positions (green) are shown in Fig. 7(d-f). Measurements of the T_e and n_e profiles were made using the 30 Hz YAG Thomson scattering system located at ϕ_{TS}=108° and an 80 channel CO_2 imaging line average density interferometer located at ϕ_{CO2}=240°.

The radial profiles of the electron density and temperature were measured at discrete time intervals with the Thomson scattering system. As shown in Fig. 8(a), the electron density inside the island O-point increases from $3.0\text{x}10^{19}$ m^{-3} at 4.066 s, just before a pellet is injected into the outer edge of the discharge, to $9.6\text{x}10^{19}$ m^{-3} at 4.100 s just after the pellet is injected. This shows that there is relatively small change in the central density when the pellet is first injected and that the peak density inside the island can exceed the central density in the discharge by at least a factor of 3. It is seen on subsequent Thomson profiles in Fig. 8(a) that some of the pellet mass diffuses into the core as the pellet is transported out of the island o-point. A characteristic flattening of the T_e profile across the island is seen in Fig. 8(b). After the pellet enters the island o-point at 4.100 s the entire T_e profile drops by about 250 eV. As the density drops in the island o-point between 4.100 and 4.153 s, T_e remains relatively constant indicating a non-adiabatic change in the pressure inside the island due to higher electron particle transport than heat transport.

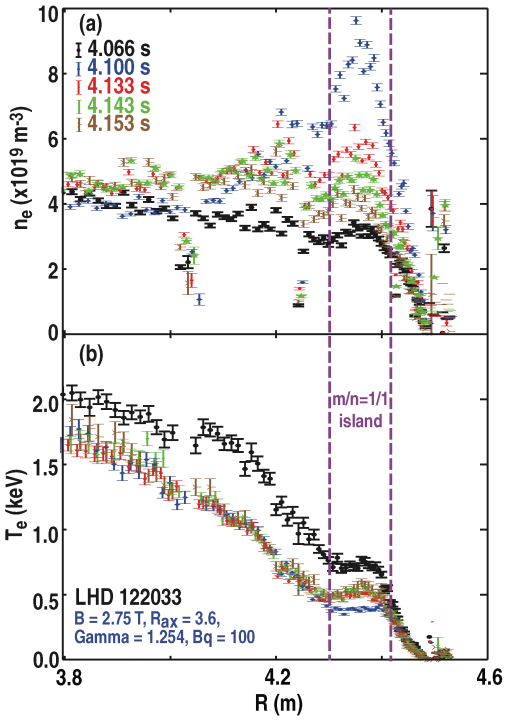

Fig. 8. Thomson scattering profiles showing the evolution of T_e and n_e following the injection of a pellet into the o-point of a m/n=1/1 island in 122033.

Figure 9 shows the differences in density response to a series of pellets injected into the island o-point in shot 122033 and into shot 122023 without an island at two radial positions R = 4.358 m (nom-inally within the island) and R = 4.117 m (radially inward from the island). These locations are shown in Figs. 7(d) and 7(f) where they are color coded to match the data in Fig. 9. The o-point injection shows a significantly larger difference between these two locations when the pellet first enters the island and the peak decreases much more rapidly than in the case without an island. In both cases there is an inward transport of the pellet mass but this transport is significantly stronger in the case without an island.

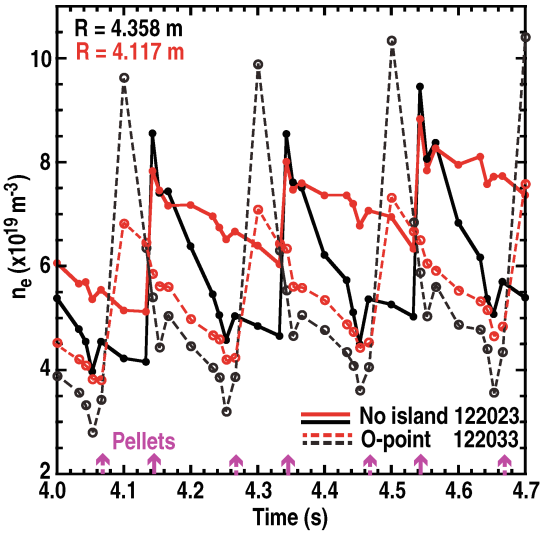

Fig. 9. Time evolution of the Thomson scattering n_e following the injection of multiple pellets into the o-point (122033) and the ×-point (122026) of an *m/n*=1/1 island located near R = 4.358 m.

4. Summary and Conclusions

In low torque, inner wall limited, DIII-D L-mode discharges, a slowly increasing (20 G/s) n=1 plasma generated magnetic field associated with a slow equilibrium evolution is locked to the applied n=1 3D field causing a large helical perturbation of the equilibrium current density and plasma pressure. The coupling of this mode to the RMP field components results in a static m/n=2/1 island with a width, based on T_e profile flattening and the MEC heat pulse transport measurements, that is about a factor of 2.9 larger than that calculated with the TRIP3D vacuum perturbation field line integration code. This suggests that the slow evolution of the plasma equilibrium and current profile results in the amplification of the island. MEC heat pulse transport measurements show a spontaneous change in the time delay across the 2/1 island along with a change in the characteristics of the ECE signal monitoring the heat pulse inside the island. These changes are consistent with a bifurcation in the topology of the edge flux surfaces inside the island from nested surfaces to a partially stochastic layer. Similar island bifurcations have been observed in LHD when the local magnetic shear across the island is changed [5] suggesting that changes in the current profile may be responsible for the bifurcation of the island topology. Transitions from L-mode confinement to an improved particle confinement (IPC) mode, triggered by the RMP field, have been observed in the DIII-D inner wall limited plasmas similar to those previously seen in TORE SUPRA [8] and TEXTOR [9]. The transition to the IPC mode is correlated with a change in the radial magnetic field associated with the n=1 kink mode component when the toroidal phase of the applied 3D perturbation field is changed by 180º.

In LHD, pellets injected into an edge m/n=1/1 island o-point result in a large increase in the density inside the island compared to that in the center of the discharge and an initial rapid transport of the pellet mass out of the island compared to a case without an island. These results indicate a reduction in the inward particle transport when the island is present.

These comparative DIII-D and LHD experiments are providing new physics insight into the effects of the coupling between ideal kink modes and magnetic islands on energy and particle transport that are beneficial for interpreting the plasma response to 3D fields in H-modes.

This material is based upon work supported by the U.S. Department of Energy, Office of Science, Office of Fusion Energy Sciences, using the DIII-D National Fusion Facility, a DOE Office of Science user facility, under Awards DE-FC02-04ER54698, DE-AC05-00OR22725, and DE-FG03-97ER54415 as well as Grant-in-Aid for Scientific research (No. 23246164) of JSPS Japan. This work is also supported by National Institute for Fusion Science (NIFS) and National Institutes of Natural Sciences (NINS) under the project of Formation of International Scientific Base and Network.

References

[1] KOMORI A., *et al.*, *Fusion Sci. Technol.* **58** (2010) 1
[2] NAGAYAMA Y., *et al.*, *Nucl. Fusion* **45** (2005) 888
[3] EVANS T.E., *et al.*, *Phys. Plasmas* **9** (2002) 4957
[4] EVANS T.E., *et al.*, *J. Nucl. Mater.* **145–147** (1987) 812
[5] IDA K., *et al.*, *New J. Phys.* **15** (2013) 013061–1–9
[6] EVANS T.E., *et al.*, "Enhanced particle flux control in a tokamak with a resonant helical divertor," in *14th EPS Conf. on Controlled Fusion and Plasma Physics, Madrid, 1987, vol. 11D, part II*, p. 770.
[7] TAKAMURA S., *et al.*, *Phys. Fluids* 30 (1987) 144
[8] EVANS T.E., *et al.*, *J. Nucl. Mater.* **196–198** (1992) 421
[9] FINKEN K.H., *et al.*, *Phys. Rev. Lett.* **98** (2007) 065001–1–4